Research Article

MOLECULAR PAIN

Molecular Pain
Volume 13: 1–17

DOI: 10.1177/1744806917704138
journals.sagepub.com/home/mpx
SAGE

Prostanoid-dependent spontaneous pain and PAR_2-dependent mechanical allodynia following oral mucosal trauma: Involvement of TRPV1, TRPA1, and TRPV4

Misa Ito[1,2], Kentaro Ono[1], Suzuro Hitomi[1], Tomotaka Nodai[1,3], Teppei Sago[4], Kiichiro Yamaguchi[1,4], Nozomu Harano[4], Kaori Gunjigake[2], Ryuji Hosokawa[3], Tatsuo Kawamoto[2] and Kiyotoshi Inenaga[1]

Abstract

During dental treatments, intraoral appliances frequently induce traumatic ulcers in the oral mucosa. Such mucosal injury-induced mucositis leads to severe pain, resulting in poor quality of life and decreased cooperation in the therapy. To elucidate mucosal pain mechanisms, we developed a new rat model of intraoral wire-induced mucositis and investigated pain mechanisms using our proprietary assay system for conscious rats. A thick metal wire was installed in the rats between the inferior incisors for one day. In the mucosa of the mandibular labial fornix region, which was touched with a free end of the wire, traumatic ulcer and submucosal abscess were induced on day 1. The ulcer was quickly cured until next day and abscess formation was gradually disappeared until five days. Spontaneous nociceptive behavior was induced on day 1 only, and mechanical allodynia persisted over day 3. Antibiotic pretreatment did not affect pain induction. Spontaneous nociceptive behavior was sensitive to indomethacin (cyclooxygenase inhibitor), ONO-8711 (prostanoid receptor EP_1 antagonist), SB-366791, and HC-030031 (TRPV1 and TRPA1 antagonists, respectively). Prostaglandin E_2 and 15-deoxy$\Delta^{12,14}$-prostaglandin J_2 were upregulated only on day 1. In contrast, mechanical allodynia was sensitive to FSLLRY-NH_2 (protease-activated receptor PAR_2 antagonist) and RN-1734 (TRPV4 antagonist). Neutrophil elastase, which is known as a biased agonist for PAR_2, was upregulated on days 1 to 2. These results suggest that prostanoids and PAR_2 activation elicit TRPV1- and TRPA1-mediated spontaneous pain and TRPV4-mediated mechanical allodynia, respectively, independently of bacterial infection, following oral mucosal trauma. The pathophysiological pain mechanism suggests effective analgesic approaches for dental patients suffering from mucosal trauma-induced pain.

Keywords

Oral traumatic mucositis, oral abscess, TRPV1, TRPA1, TRPV4, PAR_2

Date received: 13 January 2017; revised: 27 February 2017; accepted: 7 March 2017

Introduction

During dental treatments, various metal and plastic appliances are installed on the tooth or implanted in the alveolar bone. Sometimes these appliances iatrogenically induce traumatic ulcer due to mechanical stimulation and subsequently lead to painful mucositis despite considerable managements by dentists. The incidence of mucositis has been reported to be 92% in denture patients and 63%–95% in general orthodontic patients.[1–4] Implantation of miniscrews in alveolar

[1]Division of Physiology, Kyushu Dental University, Fukuoka, Japan
[2]Division of Orofacial Functions and Orthodontics, Kyushu Dental University, Fukuoka, Japan
[3]Division of Oral Reconstruction and Rehabilitation, Kyushu Dental University, Fukuoka, Japan
[4]Division of Dental Anesthesiology, Kyushu Dental University, Fukuoka, Japan

Corresponding author:
Kentaro Ono, Division of Physiology, Kyushu Dental University, 2-6-1 Manazuru, Kokurakitaku, Kitakyushu 803-8580, Japan.
Email: ono@kyu-dent.ac.jp

bone for orthodontic loading has been described to frequently cause traumatic lesions in the area in contact with the miniscrew.[5] Additionally, a clinical review has described abscess formation in orthodontic wire-induced trauma.[6] Even after removing the injurious parts of the appliance, the previously induced pain is maintained for a few days until healing, particularly during meals and conversations.[1,7,8] Some clinical studies have reported that mucosal trauma-associated pain leads to poor quality of life and decreased cooperation in therapy.[7,8] However, no studies have investigated the pathological properties and pain mechanisms responsible for mechanical trauma to the oral mucosa.

Recently, a few studies have demonstrated pain mechanisms in the oral mucosa using preclinical models of rats; the involvement of the heat-sensitive TRPV1 channel and the cold/mechanical-sensitive TRPA1 channel in nociceptive trigeminal neuronal fibers.[9,10] Incision of the buccal mucosa followed by suturing induces mechanical and heat hypersensitivities due to the upregulation of TRPV1 and/or TRPA1 channels, similar to incisions in the facial skin.[9] Oral ulcerative mucositis treated with acetic acid following the administration of 5-fluorouracil, a representative chemotherapeutic drug for head and neck cancer, induces severe spontaneous pain and mechanical allodynia due to TRPV1 activation and TRPA1 sensitization, respectively, which is dependent on bacterial infection.[10] Some differences in the pain-producing mechanisms induced by the nociceptive channels between preclinical models are probably dependent on different degrees of tissue damage and levels of infection in the oral mucosal region. In addition to TRPV1 and TRPA1, another mechano-sensitive TRP channel, TRPV4, has been reported to be involved in inflammatory pain.[11] Therefore, these channels may contribute to pain in oral traumatic mucositis.

The present study was designed to reveal cellular and molecular mechanisms associated with traumatic mucositis-induced pain in the oral mucosal region. First, we prepared a preclinical rat model for intraoral appliance-induced mucositis and evaluated the pathophysiological status. Next, we investigated spontaneous nociceptive behavior and mechanical allodynia in the preclinical model using our proprietary methods and evaluated effects of various drugs to reveal involvements of TRPV1, TRPA1, and TRPV4.

Materials and methods

Experimental animals

Male Wistar rats (eight to nine weeks of age; Kyudo, Saga, Japan) were used in this study. The rats were housed in pairs in clear cages with wood chips under specific pathogen-free conditions and maintained on a light-dark cycle (L:D, 12:12 h) in a temperature- and humidity-controlled room (21°C–23°C and 40%–60%, respectively) with food pellets and water provided ad libitum. All experiments were conducted in accordance with the National Institutes of Health guidelines (Guide for the Care and Use of Laboratory Animals) and were approved by the Animal Experiment Committee of Kyushu Dental University. All efforts were made to minimize animal suffering. Rats were randomly selected for each experiment. Measurements of all pain tests were performed in a blinded manner to the drug applications.

Model of wire-induced oral mucositis

First, in preliminary experiments, we attempted to induce traumatic mucositis by incision or mechanical scratching in the oral mucosa using a needle tip. However, the transient mechanical injuries rapidly healed by the following day, which is inconsistent with clinical pain complaints.[1,8] Hence, we selected to install a thick wire in the oral cavity for one day to generate a traumatic ulcer. An orthodontic 10-mm-length wire (E00097, TRU-CHROME, 0.018×0.025 inch [0.457×0.635 mm]; Rocky Mountain Orthodontics, Denver, CO) was manually bent into the shape shown in Figure 1(a) and soldered to a ligature wire (506-02, preformed ligature wire, 0.25 mm in diameter; TOMY International Inc., Tokyo, Japan) at the first 50°-bended angle using a spot welder (Type 660; Rocky Mountain Orthodontics). Under pentobarbital anesthesia (50 mg/kg, intraperitoneal), the inferior incisors were grooved at the top edge of the incisor gingiva (~5 mm from the tip face of the incisors) using a round diamond bur (616001-K1; MORITA, Osaka, Japan). The bent wire was installed between the incisors using the ligature wire (Figure 1(b)), and the ligation portion was completely covered with dental adhesive resin cement (Super-Bond, Sun medical, Shiga, Japan) to avoid mucosal injury at the ligation site. The free end of the thick wire, with a sharp tip generated by a wire nipper, touched the labial fornix region of the oral mucosa. As a control, a shorter thick wire (4 mm) was installed similarly without any injurious contact with the oral mucosa. To avoid detachment of the thick wires, the rats were provided with powdered food (not pellet type) during the wire installation. On the following day (day 1), the wire was removed under 2% isoflurane anesthesia. In rare cases, removal of the wire from the incisors revealed a pus discharge and bleeding from the ulcer area. Such additionally injured rats were excluded from this study.

Evaluation of oral mucositis severity

To evaluate the severity of the oral mucositis, we used the following visual oral ulcerative mucositis score,

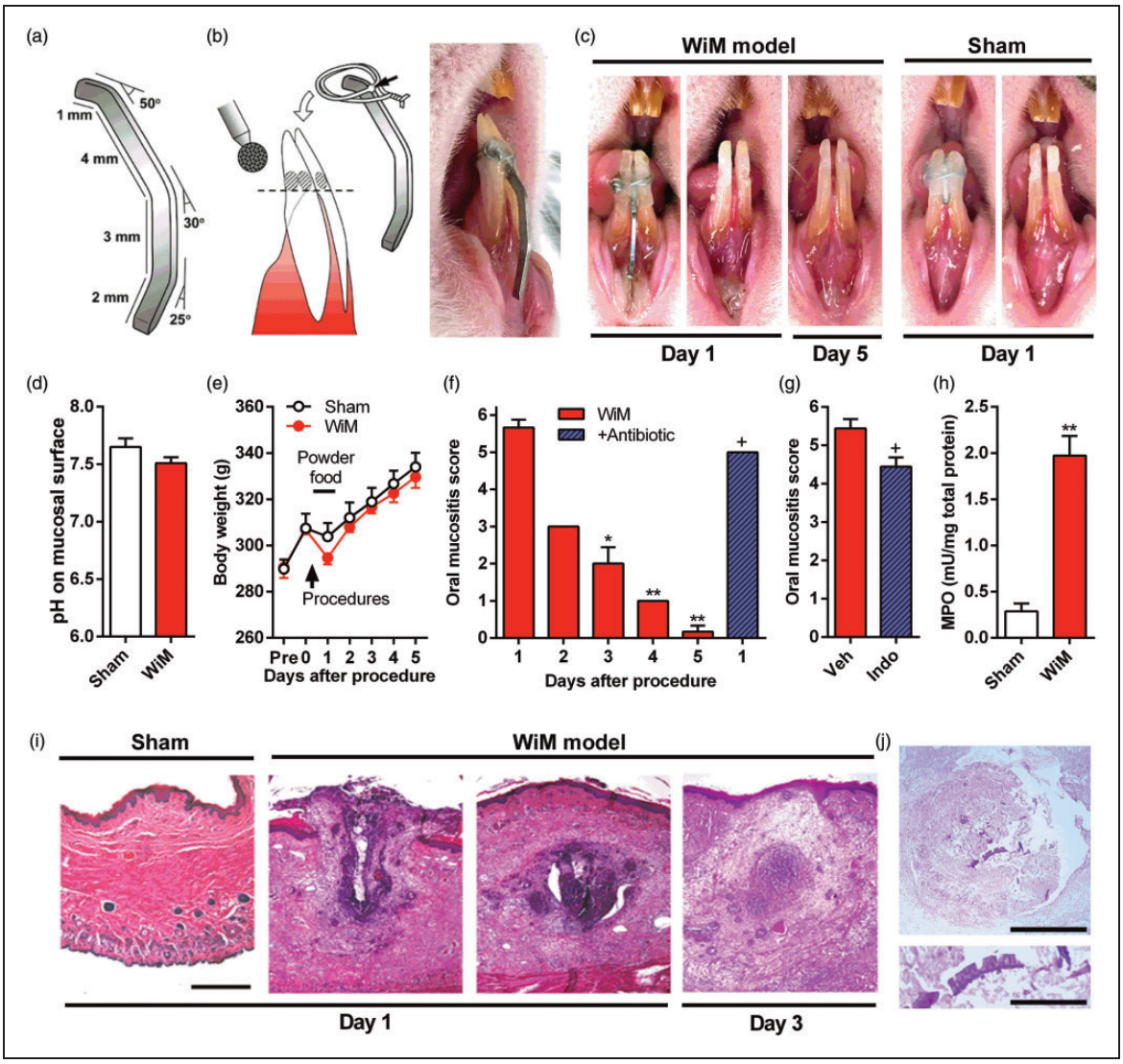

Figure 1. A rat model of wire-induced mucositis (WiM) and the pathological properties. (a) Design of the thick metal wire as an intraoral appliance in the WiM model. A 10-mm-length wire was bent three times at 50°, 30°, and 25°. (b) Procedure for installing the intraoral appliance. The inferior incisors were grooved 5 mm from the edge (horizontal dashed line) using a round diamond bur, and the bent wire was installed using the ligature wire soldered at the first angle, as indicated by a black arrow. The ligation portion is covered with dental resin cement, and the free end of the thick wire touches the labial fornix region of the oral mucosa, as shown in the photograph of the rat mouth on the right side. (c) Visual appearance of the oral mucosa of sham rats and the WiM model. For the sham, a shorter thick wire (4 mm) was similarly installed. (d) The pH of the surface of the oral mucosa in the sham and WiM model (each group, $n = 6$). (e) Daily changes in body weight following thick wire installation in the sham and WiM model (each group, $n = 5$). An arrow and horizontal bar indicate a procedure point, installation of the thick wire, and powdered food loading, respectively. (f) Daily changes in oral mucositis scores following the procedure in the sham and WiM model and effect of antibiotic pretreatment (+ antibiotic) on day 1 (each group, $n = 6$). For antibiotic pretreatment, the drinking water was supplemented with sulfamethoxazole and trimethoprim at 800 and 400 μg/mL, respectively, beginning two days prior to the procedure. * and ** indicate $P < 0.05$ and 0.01, respectively, compared with day 1; Dunnett post hoc test following one-way repeated-measures analysis of variance. $^{+}P < 0.05$ compared with day 1 without antibiotic pretreatment; Student *t* test. (g) The oral mucositis score in the WiM model on day 1 following indomethacin (Indo) pretreatment or vehicle (Veh; 0.1 M Tris-buffered saline) (each group, $n = 9$). $^{+}P < 0.05$ compared with Veh; Student *t* test. (h) Activity of the neutrophil-specific enzyme MPO in the sham and WiM model (each group, $n = 4$). $^{*}P < 0.05$ compared with the sham; Student *t* test. (i) Representative hematoxylin and eosin-stained microphotographs of the oral mucosa of sham and WiM model rats at days 1 and 3 after the procedure. Scale bar, 500 μm. Compared with the sham ($n = 5$), the oral mucosal region was largely destroyed (traumatic ulcer, left side) and formed an abscess in the submucosal layer (right side; 0.6 mm for the section shown on the left side) in WiM model rats on day 1 ($n = 5$). On day 3 ($n = 5$), the abscess trended to be reduced compared with day 1. However, we failed to detect abscess formation in any tissue sections on days 4 ($n = 2$) and 5 ($n = 2$ of 3), except for sections from a WiM model rat on day 5 with a tiny abscess (data not shown). (j) PAS staining of the abscess in the WiM model on day 1. The abscess was negative for PAS ($n = 2$), indicating that it was not a mucus cyst. The lower microphotograph is an expansion of the center of the abscess in the upper microphotograph. PAS-positive cell wall-like images. Scale bars in the upper and lower microphotographs, 300 and 100 μm, respectively.

which was modified from a previously reported score using an acetic acid-induced oral mucositis model:[10] 0, normal; 0.5, doubtful of the presence/absence of redness; 1, slight but definite redness; 2, severe redness; 3, focal pseudomembrane, without a break in the epithelium; 4, pseudomembrane, with a clear traumatic ulcer; 5, broad pseudomembrane with yellow mucus; and 6, severe swelling of the lower lip with a score level of 5. The evaluation was performed transiently under 2% isoflurane anesthesia.

Measurements of pH and temperature in the oral mucosa

Using a portable pH meter (PH-201 Z; Chemical Instruments, Tokyo, Japan) with a small electrode (CMS-30D; Chemical Instruments) and an infrared thermometer (IT-550 S; HORIBA, Kyoto, Japan), the pH and temperature on the surface of the oral mucosa was measured on day 1 under 2% isoflurane anesthesia.

Histology of the oral mucosa tissue

Under deep anesthesia with pentobarbital (100 mg/kg, intraperitoneal), the lower lip of the sham and wire-induced oral mucositis (WiM) model rats was removed and fixed in formalin. After paraffin embedding, 10-μm-thick sagittal sections of the oral mucosa were stained with hematoxylin and eosin. Periodic acid-Schiff reagent (PAS) and Alcian blue staining were performed to distinguish abscesses and mucus cysts in the submucosal layer. The sections were also stained with toluidine blue to evaluate mast cell degranulation.

To assess extravasation in the oral mucositis, WiM model rats on day 1 received Evans blue (1% in saline; E-2129; Sigma–Aldrich, St. Louis, MO) via the tail vain under deep anesthesia with pentobarbital (100 mg/kg, intraperitoneal), according to a previous study.[12] The lower lip was extracted 10 min after the administration. The tissues were fixed in 4% paraformaldehyde in phosphate-buffer, and 50-μm-thick sagittal sections were cut after paraffin embedding. The sections were observed with a stereoscopic microscope.

Myeloperoxidase activity measurements and enzyme-linked immunospecific assays

Mucosal tissue in the labial fornix region of the inferior incisors, which includes the area with the most severe mucositis, was extracted from rats that were deeply anesthetized with pentobarbital (100 mg/kg, intraperitoneal) in sham and WiM model rats on day 1 or 2. The tissue was stored at −80°C for use within three months for biochemical assays. The preserved oral mucosal tissues were melted and homogenized in PBS with 10 μM indomethacin and a protease inhibitor cocktail. Following centrifugation, the supernatants were collected, and total protein concentrations were measured using a BCA protein assay kit (Thermo Fisher Scientific, Waltham, MA). Myeloperoxidase (MPO) activity was measured using the MPO activity colorimetric assay kit (Bio Vision, Milpitas, CA). The concentrations of cyclooxygenase-2 (COX-2), prostaglandin E_2 (PGE_2), 15-deoxy-$\Delta^{12,14}$-PGJ_2 (15d-PGJ_2), interleukin-1β (IL-1β), IL-6, tumor necrosis factor-α (TNF-α), bradykinin, and neutrophil elastase in the supernatants were measured with the following ELISA kits: Rat COX-2 Assay Kit (27187; IBL International, Hamburg, Germany), Prostaglandin E_2 ELISA Kit (ab133021; Abcam, Cambridge, MA), 15-deoxy-delta^{12,14}-PGJ_2 ELISA Kit (ab133031, Abcam), Rat IL-1 beta, IL-6 and TNFα ELISA Kits (ER2IL1B, ER3IL6, and ER3TNFA, respectively; Thermo Fisher Scientific), Bradykinin ELISA Kit (ab136936; Abcam) and Rat HNE/Neutrophil Elastase ELISA Kit (LS-F20775; LifeSpan BioScience, Inc., Seattle, WA). The assays were performed in duplicate, and the concentrations and enzyme activities were standardized based on the total protein concentrations.

Quantification of bacterial counts

On day 1, the mucosal tissues of the sham and the WiM model with and without antibiotic pretreatment were extracted from rats that were deeply anesthetized with pentobarbital (100 mg/kg, intraperitoneal). All instruments and the entire lower lip skin were sterilized with 70% ethanol before each preparation, and the superficial skin was carefully removed with scissors before removing the lower lip. The isolated lip was trimmed to construct a block with a mucosal surface of approximately 3 × 3 mm and a thickness of 1–2 mm. The block was then bisected with a surgical scalpel. The divided mucosal tissue was placed into a pre-weighed 1.5-mL plastic tube filled with 1 mL of sterilized PBS and ultra-sonicated for 30 s (38 kHz, US-2; SND, Nagano, Japan) to leach out oral bacteria. Each sample (50 μL) was plated in duplicate onto Brain Heart Infusion agar (Nissui, Tokyo, Japan), not exceeding 500 counts/90-mm-diameter dish. Anaerobic incubation was performed in an airtight container with AnaeroPack-Anaero, an O_2-absorbing and CO_2-generating agent (Mitsubishi Gas Chemical, Saga, Japan), followed by overnight incubation at 37°C. The colony-forming units (CFUs) of the duplicated bacterial culture plates were then manually counted. The number of CFUs is presented as the number per wet tissue weight.

Drug applications

In this study, four kinds of drug applications were performed: (1) administration of fluids, (2) intraperitoneal

administration, (3) swab application, and (4) submucosal injection.

As antibiotic pretreatment for the WiM model, sulfamethoxazole (Wako, Osaka Japan) and trimethoprim (MP Biomedicals, Illkirch, France) were dissolved in drinking water at 800 and 400 μg/mL, respectively. The pretreatment was performed beginning at two days prior to the wire installation and continued for five days. The pretreatment revealed a significant efficacy for blocking bacterial loading in oral ulcer models of rats.[10]

As an anti-inflammatory pretreatment, the nonselective COX inhibitor indomethacin (Wako) was intraperitoneally administered at 5 mg/5 mL/kg. The drug administration was performed once per day on days 0 and 1 (4–6 hr prior to the pain tests). As a control, the same volume of a vehicle solution (0.1 M Tris-buffered saline) was administered. The pretreatments revealed a significant efficacy for PGE_2 production in oral ulcer models of rats in our previous studies.[10,13,14]

To suppress TRPV1, TRPA1, and TRPV4 activation in the WiM model, the TRPV1-selective antagonist SB-366791 (Wako), the TRPA1-selective antagonist HC-030031 (Wako), and the TRPV4-selective antagonist RN-1734 (EMD Millipore, Billerica, MA) were intraperitoneally administered at 1, 10 and 10 mg/4 mL/kg, respectively, 30 min before the pain tests (30 min after removing the thick wire on day 1). The concentrations of the antagonists were determined according to previous studies.[10,15] As a control, the same volume of a vehicle solution (10% dimethylsulfoxide [DMSO]-containing saline) was administered.

To examine the local pain mechanism in the oral mucositis area, drugs were applied to the WiM region for 5 min under 2% isoflurane anesthesia immediately after removing the thick wire (1 hr prior to the pain tests), using a swab soaked with the drug solutions (in saline). The concentrations of the PGE_2 receptor EP_1 antagonist ONO-8711 (Cayman Chemical, An Arbor, MI) and the PAR_2 antagonist FSLLRY-NH_2 (TOCRIS, Bristol, UK) were 0.5 and 2.0 mg/mL, respectively, according to previous studies.[16,17] The concentrations of SB-366791, HC-030031, and RN-1734 were 0.25, 2.5, and 2.5 mg/mL, respectively. According to our previous study,[10] the non-membrane permeable TRPV1/TRPA1 pore passing anesthetic QX-314 was used at 1%. As controls, vehicle solutions were applied (saline for FSLLRY-NH_2 and QX-314; 10% DMSO-containing saline for the other drugs).

To examine whether oxidation, ATP and TRP channels mediate mechanical pain in WiM, the anti-oxidant α-lipotic acid (α-LA; 0.5 mg/mL; Wako), the P2X3 and P2X2/3 antagonist A-317491 (2 mM; Sigma–Aldrich) and the non-selective TRP and Ca^{2+} channel antagonist ruthenium red (RuR; 2.4 mM; Wako) was injected into the labial fornix region of the inferior incisors in 10 μL saline in WiM model rats under 2% isoflurane anesthesia immediately after removing the thick wire (1 hr prior to the pain tests), using a 30-G needle with a 50-μL Hamilton syringe (Hamilton, Reno, NV). RN-1734 was similarly injected into the same region in WiM model rats on day 2 after measuring pre-value of mechanical threshold. The concentrations of α-LA, A-317491, and RuR were determined according to previous studies,[10,18,19] and that of RN-1734 was the same as the swab application. As a control, a vehicle solution (saline) was applied.

To examine whether the interaction of PAR_2 and TRPV4 in the oral mucosa, elastase (Roche, Basel, Switzerland) and GSK1016790A (Cayman Chemical) were similarly injected at 10 μg/mL and 5 μg/μL, respectively, in 10 μL saline in naive rats under 2% isoflurane anesthesia, after measuring pre-value of mechanical threshold. The concentrations of GSK1016790A and elastase were determined according to previous studies.[20,21] GSK1016790A was diluted 100-times in ethanol, while the other drugs were diluted 10-times in DMSO. RN-1734 and FSLLRY-NH_2 were coinjected with elastase to block TRPV4 and PAR_2 activation, respectively. The concentrations of RN-1734 and FSLLRY-NH_2 were the same as the swab application. As a control, a vehicle solution (1% ethanol- and 10% DMSO-containing saline) was applied.

Behavioral observation of mouth rubbing

Mouth rubbing with both forelimbs was measured over a constant time period (between 4 and 6 p.m.) as an orofacial nociceptive behavior.[22] Prior to the measurements, all rats were acclimated over a period of three days (once per day) to the plastic cage (30 × 30 × 30 cm) used for the observations. To evaluate spontaneous pain, the behavioral observation was performed for 10 min.

Withdrawal threshold to von Frey stimulation

Using the stable intraoral opening (SIO) method, the rats were pierced with a magnetized ring in the lower lip to stably expose the oral mucosa in the labial fornix region of the inferior incisors, as described in detail in our previous study.[22] First, in rats anesthetized with pentobarbital (50 mg/kg, intraperitoneal), a magnetized needle (the equivalent of 22 gauge, Daiso Sangyo, Hiroshima, Japan) was used to pierce the mentum skin below the lower lip of the rat. The needle was then bent into a ring, and the tip of the needle was removed. One week after piercing, the rats were trained for 10 min per day to stably protrude their perioral regions through a hole in a hand-made restrainer. After demonstrating stable behavior in the restrainer (~three to four days after the initiation of training), the rats were further trained to expose

the oral mucosa. A small neodymium magnet (3 mm in diameter; Waki, Osaka, Japan), which was attached to a 4-g weight by a string, was attached to the pierced ring, resulting in a constant vertical pressure. When the rats flicked away and backed up, the magnet was released from the ring without damage to the pierced region. The following intraoral behavioral test was performed after confirming that each rat had adapted to the experimental conditions (~two to three weeks after piercing).

The head withdrawal threshold to mechanical stimulation was measured in the oral mucosa by applying von Frey filaments (0.02–6 g filaments, North Coast Medical, Morgan Hill, CA, and 0.2 and 0.3 g handmade filaments). These mechanical stimulations were applied to the oral mucosa in the labial fornix region of the inferior incisors, which involved oral mucositis in the WiM model. The head withdrawal threshold was defined as the minimum pressure required to evoke an escape. Each measurement was repeated five times at 3–4-min intervals, and the measurements were averaged following exclusion of the maximum and minimum values.[13,23–25]

Real-time reverse transcription-polymerase chain reaction

Bilateral trigeminal ganglions were extracted from sham and WiM model rats on day 1 under deep anesthesia with pentobarbital (100 mg/kg, intraperitoneal), immediately transferred to ISOGEN (Wako) and frozen at −80°C. After homogenization of the trigeminal ganglion tissues of the third branch, which innervates the lower lip, total RNA was extracted using the RNeasy Mini Kit (Qiagen, Tokyo, Japan) and reverse-transcribed with random hexamers (Applied Biosystems, Foster, CA). Four replicates from four rats were assessed for each group. A 1.5-μl cDNA aliquot was amplified in a 7300 Real Time PCR System (Thermo Fisher Scientific) according to the manufacturer's recommendations with THUNDERBIRD SYBR qPCR Mix (Toyobo, Osaka, Japan). The following primers were used: PTGER1 (EP_1 gene), 5′-GGGCATCATGGTGGTTTC-3′ and 5′-GC CAACACCACCAATACCA-3′; F2RL1 (PAR_2 gene), 5′-GGCTGCTGGGAGGTATCAC-3′ and 5′-CGTGT CCAATCTGGCCAATC-3′; TRPV1, 5′-CAACAGGA AGGGGCTCAC-3′ and 5′-TCTGGAGAATGTAGGC CAAGAC-3′; TRPA1, 5′-ATTTGCGGCCCTGAG TTTTT-3′ and 5′-GCGTACATCCATCATTGTCCT-3′; TRPV4, 5′-CCACCCCAGTGACAACAAG-3′ and 5′-GAGCTTTGGGGCTCTGTG-3′; β-actin, 5′-CCCG CGAGTACAACCTTCT-3′ and 5′-CGTCATCCATG GCGAACT-3′. The assays were performed in duplicate, and the ΔΔCT method was used to quantify the relative expression. There were no differences in the CT values (the cycle number when the fluorescent signal crosses the detection threshold) for β-actin between the two animal groups (data not shown). Hence, the given relative amount for each sample was standardized to that of β-actin, and the ratios were calculated relative to the average value for the naive group.

Ca^{2+} imaging for trigeminal ganglion neurons

After deep anesthetization with pentobarbital (100 mg/kg, intraperitoneal), the bilateral trigeminal ganglions of naive rats was removed, minced, and incubated in collagenase (2 mg/mL; Wako) and dispase (0.2 mg/mL; Sanko, Tokyo, Japan) in Ca/Mg-free HBSS for 1 h, as previously described.[21] To remove debris, digested cell suspensions were centrifuged on 30% Percoll (Sigma–Aldrich). After washing, the cell pellet was resuspended in L-15 Lebovitz medium (Thermo Fisher Scientific) with antibiotic/antimycotic solution (0.1%), and the cells were plated on glass bottom dishes that had been coated with poly-ornithine and laminin. The plated cells were incubated at 37°C in a humidified chamber. To avoid the effects of culture and neurotrophin on cell properties,[26,27] this study was performed using a short duration culture (3–8 h after cell plating) without any neurotrophins.

Before recording, trigeminal ganglion cells were incubated with fura-2AM (10 μM, Dojindo, Kumamoto, Japan) at 37°C for 30 min. The dishes were mounted on the stage of an inverted fluorescence microscope (IX71, Olympus, Tokyo, Japan) and washed with culture medium using a perfusion solution (mM): NaCl 130, KCl 5, $MgCl_2$ 1, $CaCl_2$ 2, glucose 10, and HEPES 10 (pH 7.4, adjusted with NaOH). The fura-2 was excited every 2 s by alternate illumination with 340 and 380 nm light using a Ca^{2+} imaging system (Hamamatsu Photonics, Hamamatsu, Japan). GSK1016790A, the TRPA1 agonist allyl isothiocyanate (AITC), and the TRPV1 agonist capsaicin (CPS) were diluted as stock solutions in ethanol and then further diluted 100-fold to 100 nM, 1 mM and 1 μM, respectively, with the perfusion solution. All drugs were applied for 2 min by bath application. To confirm whether the recorded cells were neurons, 50 mM KCl-supplemented perfusion solution was consistently applied at the end of the recordings. All Ca^{2+} responses are expressed as a ratio (F340/F380), and the recorded cells were deemed to be sensitive to drug if they provided values of more than 0.01 for the Δ ratio after application. In a preliminarily experiment, 1% ethanol-containing solution did not change the ratio compared with the baseline (data not shown).

Statistical analysis

Data are presented as the mean ± SEM, and n represents the number of rats tested. An unpaired Student t test was used to compare differences between two different

groups or experimental days. To compare between-group differences in the number of CFUs, the Mann-Whitney U test was used. Following two-way repeated-measures analysis of variance, the Sidak post hoc test was applied to analyze daily or time changes between two different groups. Dunnett post hoc test was applied following one-way repeated-measures analysis of variance to analyze three or more groups. Significance was accepted at $P < 0.05$.

Results

Generation of the WiM model

On the following day (day 1) from installation of a bent wire, a clear traumatic ulcer was caused at the other free end of the wire-touched mucosal area of the labial fornix, as shown in Figure 1(c). The traumatic ulcer was limited to the region in contact with the wire, which differed visually from the acetic acid-induced ulcerative mucositis following dermis exposure due to peeling of the mucosal membrane in our previous studies.[10,22] There were no lesions or mucositis in other mucosal areas. The rat model used in this study is termed the "WiM (wire-induced mucositis) model." The sham procedure did not cause any lesions in the oral mucosa (Figure 1(c)), emphasizing that ligation of the thick wire had no injurious effects on the oral mucosa. In preliminarily experiments, we failed to generate a traumatic ulcer on the day after creating a transient incision and applying mechanical scratching in the oral mucosa using a needle tip in four and three rats, respectively. Therefore, persistent mechanical injury to the oral mucosa seemed to be necessary to develop traumatic mucositis.

The installed wires were removed on day 1 under isoflurane anesthesia, carefully to avoid additional injury by the free end of the wire. The mucosal lesion exhibited a crude surface that was slightly covered with clear yellow mucus (Figure 1(c)). On the surface of the traumatic ulcer, the pH was not significantly changed, relative to that in healthy oral mucosa of the sham (Figure 1(d)). There was no difference in mucosal temperature ($33.6 \pm 0.7^{\circ}C$ and $33.4 \pm 0.3^{\circ}C$, respectively). In addition, there was no significant difference in change of body weight between the sham and WiM model, although the body weight of the WiM model on day 1 trended to lower than that of the sham (Figure 1(e)). The absence of an increment of body weight in sham rats on day 1 probably resulted from the wire installation procedure and powder food loading (to avoid detachment of the appliance).

The mean oral mucositis score of 5.7 on day 1 rapidly decreased to 3 on day 2 (Figure 1(f)), indicating a disappearance of the traumatic ulcer on day 2. Gradually, the mucositis was cured over five days (Figure 1(c)); the oral mucositis scores decreased each day (Dunnett post hoc test, $P < 0.05$ on day 3 and $P < 0.01$ on days 4 and 5, compared with day 1; Figure 1(f)). On day 1, the antibiotic and anti-inflammatory (indomethacin) pretreatments slightly decreased to a score of 5 and 4.3, respectively (t test, $P < 0.05$ for both treatments; Figure 1(f) and (g)). Such limited efficacies of both the antibiotic and indomethacin pretreatments for oral mucositis severity have been similarly observed in the 5-fluorouracil-administered oral ulcerative mucositis model.[10]

MPO activity was significantly elevated in the WiM model compared with the sham, suggesting leukocyte infiltration into the oral mucosa of the model (t test, $P < 0.01$; Figure 1(h)). In the ELISA assays, IL-1β, IL-6, and TNF-α were upregulated on day 1 in the WiM model relative to the sham (t test, $P < 0.01$ for IL-1β and $P < 0.05$ for IL-6 and TNF-α; Supplementary Figure 1(a)–(c)). However, there was no significant difference in bradykinin, which is a well-known inflammatory pain inducer,[11] between the sham and WiM model (Supplementary Figure 1(d)).

Histological appearance

The histological assessment revealed an obvious traumatic ulcer and mucosal swelling of the oral mucosal tissue in the labial fornix region in the WiM model on day 1 relative to the sham (Figure 1(i)), consistent with the visual oral mucositis score (Figure 1(f)). Furthermore, the histology demonstrated the formation of a clear abscess, which formed with leukocyte accumulation, of more than 1 mm in the submucosal area, in addition to broad inflammatory cell invasion (Figure 1(i)). The histological structure was further confirmed as an abscess based on negative images with PAS staining (Figure 1(j)) and Alcian blue staining (data not shown), which detects the mucus cyst. Such abscess formation has been suggested in a clinical review.[6] The abscess was gradually reduced each day (Figure 1(i)), and it difficult to detect on days 4 and 5.

PAS staining revealed PAS-positive cell wall-like particles in the center of the abscess, which were derived from sawdust and powdered foods (inset microphotograph of a high-power field; Figure 1(j)). However, abscess formation was observed even under experimental conditions without sawdust and powdered foods and after antibiotic pretreatment (data not shown), suggesting that it was primarily derived from damaged host cells rather than non-host materials, oral bacteria, and food.

After tail vein injection of Evans blue, the submucosal area involving the abscess on day 1 was stained with the drug (data not shown), suggesting a high level of extravasation in traumatic mucositis, including the abscess. To examine the involvement of mast cell degranulation in

the oral mucositis, the oral mucosal tissue sections of the labial fornix region were stained with toluidine blue. Many toluidine blue-positive granule-containing mast cells were detected in the submucosal layer of the healthy oral mucosa, but such toluidine blue-positive cells were rarely detected around the traumatic ulcer and abscess in the WiM model (Supplementary Figure 1(e)), indicating exhaustion of the mast cell granules.

Spontaneous pain and mechanical allodynia

Spontaneous pain was evaluated by quantifying the spontaneous mouth rubbing behaviors for 10-min periods, and mechanical allodynia was evaluated based on the head withdrawal threshold by von Frey filaments using the SIO method, which is a proprietary assay system for conscious rats.[10,22] Figure 2(a) and (b) shows the daily changes in spontaneous mouth rubbing and the head withdrawal threshold, respectively, in sham and WiM model rats. After removing the thick wire, relative to the sham, WiM model rats showed increased spontaneous mouth rubbing, peaking on day 1 (Sidak post hoc test, $P < 0.01$) followed by a rapid recovery to pretreatment levels on day 2 (Figure 2(a)), and reduced head withdrawal thresholds, peaking on day 1 (Sidak post hoc test, $P < 0.01$ on days 1 and 2 and $P < 0.05$ on day 3) and gradually recovering to control levels up to day 4 (Figure 2(b)). These results suggest the induction of spontaneous pain and mechanical allodynia in the WiM model.

Importantly, in contrast to the model of acetic acid-induced oral ulcerative mucositis,[10] antibiotic pretreatment did not significantly suppress the induction of spontaneous pain and mechanical allodynia in the WiM model (Figure 2(a) and (b)). To examine the impact of bacterial loading, we quantified bacterial infections in the traumatic ulcerative region in the model. The numbers of CFUs under aerobic and anaerobic conditions on day 1 were significantly increased approximately 100-fold compared with the healthy oral mucosa of the sham (Mann-Whitney U test, $P < 0.05$ for both conditions), and the increments were suppressed by antibiotic pretreatment (Mann-Whitney U test, $P < 0.05$ for both conditions) (Figure 2(c)). Together with the decrease in the oral mucositis score following antibiotic pretreatment, these results indicated that the antibiotic pretreatment was effective for the suppression of bacterial infection. In previous studies investigating infectious inflammatory pain,[10,28] spontaneous pain, and/or mechanical allodynia were induced from over 10^4 CFU per milligram of tissue. Therefore, in this study, the number of CFUs in tissue was regarded as the pain-producing level. The increment levels of bacterial loading in the WiM model were insufficient to generate a pain-producing level (Figure 2(c)).

Spontaneous pain mechanism

The anti-inflammatory pretreatment using the COX-1/2 inhibitor indomethacin significantly inhibited the

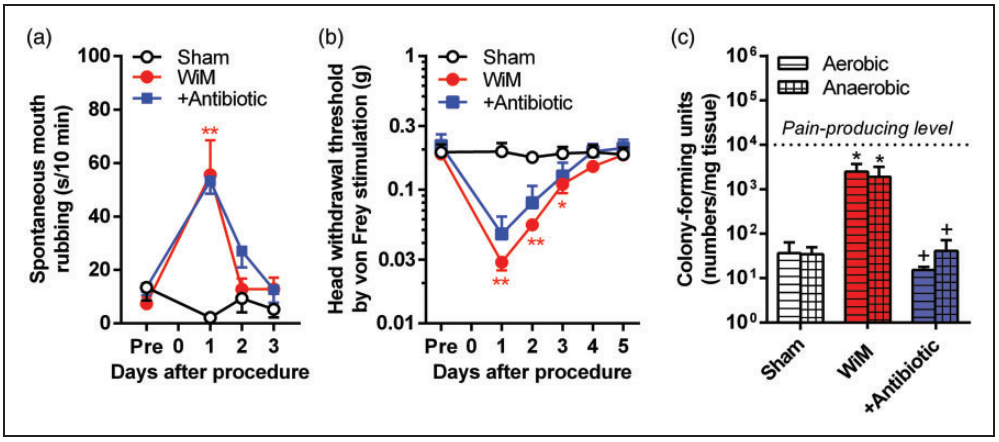

Figure 2. Spontaneous pain and mechanical allodynia induction in the wire-induced mucositis (WiM) model and effect of antibiotic pretreatment. As the antibiotic pretreatment, sulfamethoxazole- and trimethoprim-containing drinking water was supplemented beginning two days prior to the procedure (installation of the thick wire) and continued for five days. (a) Daily changes in spontaneous mouth rubbing periods in the sham and model rats with or without antibiotic pretreatment ($n = 5$, 4, and 5, respectively). (b) Daily changes in the head withdrawal threshold by von Frey stimulation in sham and model rats with or without antibiotic pretreatment ($n = 5$, 4, and 5, respectively). In (a) and (b), * and ** indicate $P < 0.05$ and 0.01, respectively, compared with the sham; Sidak post hoc test following two-way repeated-measures analysis of variance. (c) The numbers of CFU under aerobic and anaerobic conditions in extracted oral mucosal tissues (each group, $n = 4$). The horizontal dashed line in the graph indicates the pain-producing level, according to previous studies investigating bacterial infection-induced pain.[10,28] $^*P < 0.05$ compared with sham; $^+P < 0.05$ compared without antibiotic pretreatment in the WiM model; Mann-Whitney U test.

increase in spontaneous mouth rubbing on day 1 in the WiM model (*t* test, $P < 0.05$; Figure 3(a)). Consistently, the inflammation regulatory enzyme, COX-2, was upregulated on day 1 in the WiM model relative to the sham (*t* test, $P < 0.05$; Figure 3(b)). Furthermore, swab application of the PGE_2 receptor subtype 1 EP_1-selective antagonist, ONO-8711, significantly inhibited the increase in spontaneous mouth rubbing on day 1 in the WiM model (*t* test, $P < 0.05$; Figure 3(c)). To confirm the production of prostanoids, we measured the contents of PGE_2 and 15d-PGJ_2 in the oral mucosal regions of sham and WiM model rats on day 1 and/or 2 by ELISA. The 15d-PGJ_2 is a cyclopentenone PG that is produced by dehydration within the cyclopentane ring of PGD_2.[29] The two distinctly formed prostanoids were significantly upregulated in the WiM model on day 1 relative to the sham (Dunnett post hoc test, $P < 0.01$ in PGE_2 and $P < 0.05$ in 15d-PGJ_2), and the increments were decreased on day 2 to levels mimicking the sham (Figure 3(d) and (e)). Thus, the time course and drug sensitivities of spontaneous pain induction were consistent with those of prostanoid production.

PGE_2 injection induces TRPV1-, TRPA1-, and TRPV4-mediated pain, and cyclopentenone PGs directly activate TRPA1.[29–32] Therefore, to examine the involvements of the nociceptive TRP channels in spontaneous pain following mechanical trauma, we investigated the effects of the TRPV1, TRPA1, and TRPV4 antagonists, SB-366791, HC-030031, and RN-1734, respectively, on spontaneous mouth rubbing in the WiM model.

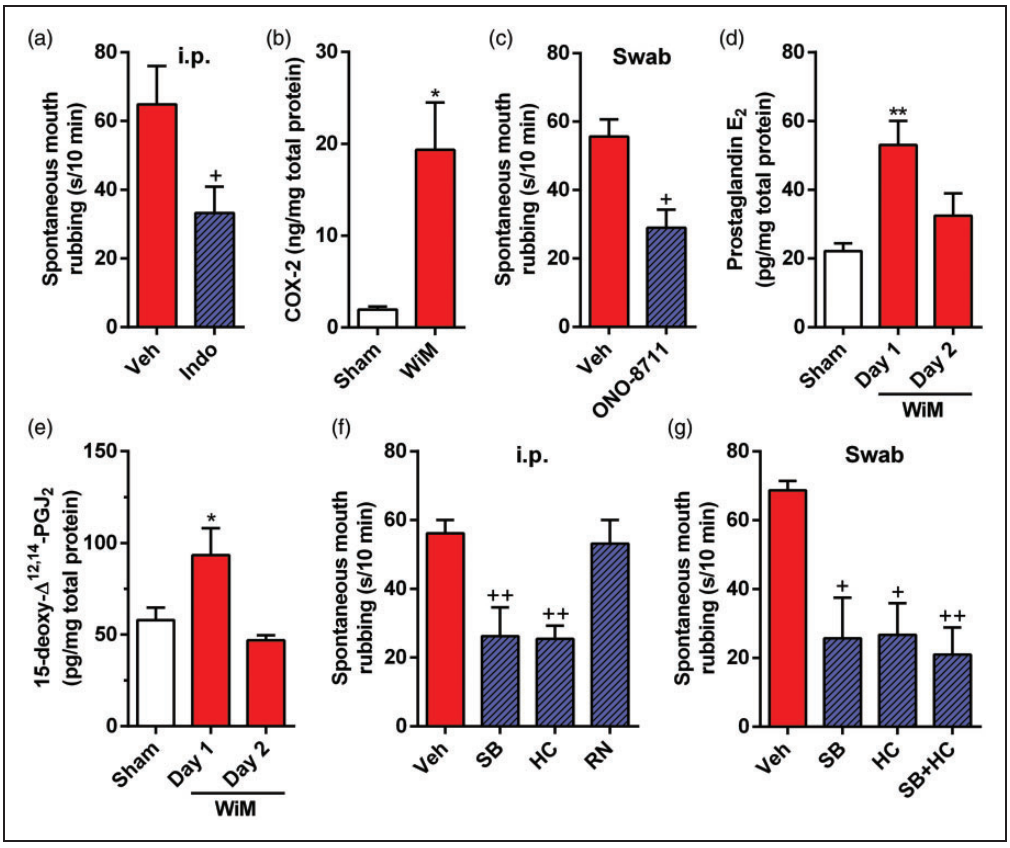

Figure 3. Mechanism underlying spontaneous pain in the wire-induced mucositis (WiM) model. (a) Spontaneous mouth rubbing after intraperitoneal (i.p.) indomethacin pretreatment (Indo) and vehicle (Veh; 0.1 M Tris-buffered saline) on day 1 (each group, $n = 9$). $^{+}P < 0.05$ compared with Veh; Student *t* test. (b) Cyclooxygenase-2 (COX-2) level in the oral mucosa of sham and WiM on day 1 (each group, $n = 4$) by ELISA. $^{*}P < 0.05$ compared with the sham; Student *t* test. (c) Spontaneous mouth rubbing after swab application of the EP_1 antagonist ONO-8711 and Veh (10% dimethylsulfoxide [DMSO] -containing saline) on day 1 (each group, $n = 6$). $^{+}P < 0.05$ compared with Veh; Student *t* test. (d and e) Prostaglandin E_2 and 15-deoxy-$\Delta^{12,14}$-PGJ_2 (known as a TRPA1 agonist) levels in the oral mucosa of the sham on day 1 and the WiM model on days 1 and 2 (each group, $n = 4$) by ELISA. * and ** indicate $P < 0.05$ and 0.01, respectively, compared with the sham on day 1; Dunnett post hoc test following one-way repeated-measures analysis of variance (ANOVA). (f) Spontaneous mouth rubbing after i.p. administration of SB-366791 (SB: a TRPV1 antagonist), HC-030031 (HC: a TRPA1 antagonist), RN-1734 (RN: a TRPV4 antagonist), and Veh (10% DMSO-containing saline) in the WiM model on day 1 (each group, $n = 5$). $^{++}P < 0.01$ compared with Veh; Dunnett post hoc test following one-way repeated-measures ANOVA. (g) Spontaneous mouth rubbing after swab application of SB, HC alone, a mixture of SB and HC (SB + HC) and Veh (10% DMSO-containing saline) in the WiM model on day 1 (each group, $n = 5$). $^{+}$ and $^{++}$ indicate $P < 0.05$ and 0.01, respectively, compared with Veh; Dunnett post hoc test following one-way repeated-measures ANOVA.

The increase in spontaneous pain on day 1 was suppressed by intraperitoneal administrations of SB-366791 and HC-030031 (Dunnett post hoc test, $P < 0.01$ for both drugs) but not by RN-1734 (Figure 3(f)), suggesting a dependency of TRPV1 and TRPA1 channel opening and TRPV4 channel closing in the WiM model. Furthermore, swab application of either or both SB-366791 and HC-030031 to the traumatic ulcer region for 5 min significantly suppressed the spontaneous pain (Dunnett post hoc test, $P < 0.05$ for SB-366791 and HC-030031 alone and $P < 0.01$ for a mixture of SB-366791 and HC-030031; Figure 3(g)). The significant efficacies of SB-366791 and HC-030031 in the swab application suggest that TRPV1 and TRPA1 activation are induced peripherally in traumatic mucositis in this model.

Mechanism of mechanical allodynia

In contrast to spontaneous pain, mechanical allodynia in the WiM model on day 1 was resistant to pretreatment with indomethacin (Figure 4(a)). Furthermore, the mechanical allodynia was not inhibited by submucosal injections of the reactive oxygen species inhibitor α-LA and the nociceptive ionotropic ATP receptor P2X3 and P2X2/3 antagonist A-317491, while it was significantly improved by the non-selective TRP channel antagonist RuR (Figure 4(b)). These results suggest that there is no involvement of the COX pathway, reactive oxygen species, or ATP in mechanical allodynia. Based on the lack of efficacy of the antibiotic pretreatment (Figure 2(a) and (b)), bacterial toxins (lipopolysaccharide and *N*-formyl peptides), which have been identified to induce

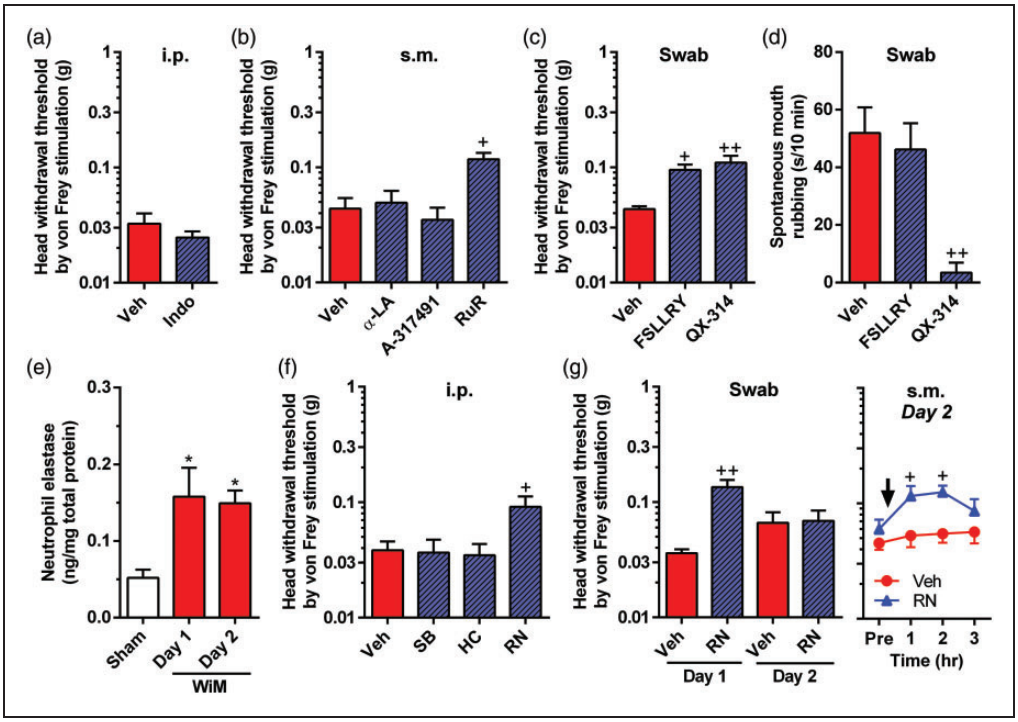

Figure 4. Mechanism underlying mechanical allodynia in the wire-induced mucositis (WiM) model and effects of PAR_2 antagonist and QX-314 on spontaneous pain. (a) Head withdrawal threshold by von Frey filaments after intraperitoneal (i.p.) indomethacin pretreatment (Indo; $n = 4$) and vehicle (Veh, $n = 5$; 0.1 M Tris-buffered saline) on day 1. (b) Head withdrawal threshold by von Frey filaments after submucosal (s.m.) injections of α-lipotic acid (α-LA: an anti-oxidant drug, $n = 4$), A-317491 (a P2X3 and P2X2/3 antagonist, $n = 4$), ruthenium red (RuR, $n = 6$) and vehicle (Veh, saline; $n = 7$) on day 1. $^{+}P < 0.05$ compared with Veh; Dunnett post hoc test following one-way repeated-measures analysis of variance (ANOVA). (c and d) Head withdrawal threshold by von Frey filaments and spontaneous mouth rubbing, respectively, after swab applications of the PAR_2 antagonist FSLLRY-NH_2 (FSLLRY; $n = 4$), QX-314 ($n = 4$) and Veh (saline, $n = 6$) on day 1. $^{+}$ and $^{++}$ indicate $P < 0.05$ and 0.01, respectively, compared with Veh; Dunnett post hoc test following one-way repeated-measures ANOVA. (e) Neutrophil elastase level in the oral mucosa of sham and WiM on days 1 and 2 (each group, $n = 4$–6) by ELISA. $^{*}P < 0.05$ compared with the sham on day 1; Dunnett post hoc test following one-way repeated-measures ANOVA. (f) Head withdrawal threshold by von Frey filaments after i.p. administrations of SB-366791 (SB: a TRPV1 antagonist), HC-030031 (HC: a TRPA1 antagonist), RN-1734 (RN: a TRPV4 antagonist), and Veh (10% dimethylsulfoxide [DMSO]-containing saline) (each group, $n = 5$). $^{+}P < 0.05$ compared with Veh; Dunnett post hoc test following one-way repeated-measures ANOVA. (g) Head withdrawal threshold by von Frey filaments after swab application of RN and Veh on days 1 and 2 and s.m. injection of RN and Veh on day 2 (each group, $n = 5$). In the swab application (left side), $^{++}P < 0.01$ compared with Veh; Dunnett post hoc test following one-way repeated-measures ANOVA. In the s.m. injection (right side), $^{+}P < 0.05$ compared with Veh; Sidak post hoc test following two-way repeated-measures ANOVA.

mechanical allodynia in a 5-fluorouracil-administered oral ulcerative mucositis model,[10] might not largely contribute to mechanical allodynia in the WiM model. Another possibility was the activation of PAR_2 because of its abundant expression in sensory neurons and involvement in inflammatory pain.[11,33] Swab application of the PAR_2 selective antagonist FSLLRY-NH_2 significantly increased the declined head withdrawal threshold in the model compared with the vehicle (Dunnett post hoc test, $P < 0.05$; Figure 4(c)). The same application did not alter the increase in spontaneous mouth rubbing (Figure 4(d)). Due to the granule exhaustion in mast cells on day 1, there was very little involvement of mast cell-derived serine protease tryptase, potentially causes PAR_2 activation.[34] Recently, neutrophil elastase has been reported as a biased PAR_2 agonist.[21] It is possible that the enzyme is abundant in the traumatic mucositis of the WiM model because of the accumulation of neutrophils (abscess formation) for a few days (Figure 1(i)), consistent with the duration of mechanical allodynia induction (Figure 2(b)). As expected, a significant upregulation of neutrophil elastase was detected in the WiM model, not only on day 1 but also day 2 (Dunnett post hoc test, $P < 0.05$ for both days; Figure 4(e)).

To examine the involvements of the nociceptive TRP channels in mechanical allodynia following mechanical trauma, we investigated the effects of the TRP channel subtype specific antagonists, SB-366791, HC-030031, and RN-1734, on head withdrawal threshold in the WiM model on day 1 and/or 2. The declined head withdrawal threshold on day 1 was suppressed by systemic administration of RN-1734 (Dunnett post hoc test, $P < 0.05$) but not by those of SB-366791 and HC-030031 (Figure 4(f)). Furthermore, swab application of RN-1734 to the traumatic ulcer region for 5 min significantly suppressed mechanical allodynia on day 1 (Dunnett post hoc test, $P < 0.01$) but not on day 2 (Figure 4(g)). Because the ulcer in the model quickly disappeared by day 2 (Figure 1(f)), the drug in the swab might be insufficient to permeate the deeper mucosal area on that day. To exert sufficient efficacy of the drug in the target tissue, we submucosally injected RN-1734 on day 2. The submucosally injected RN-1734 significantly increased the head withdrawal threshold 1 and 2 h compared with vehicle injection (Sidak post hoc test, $P < 0.05$ for both time points; Figure 4(g)).

Elastase-induced TRPV4-mediated mechanical allodynia in naive rats

In naive rats, submucosal injection of the TRPV4-selective agonist GSK1016790A significantly reduced the head withdrawal threshold 1 h after the injection compared with the vehicle injection (Sidak post hoc test, $P < 0.01$; Figure 5(a)). Submucosal injection of elastase significantly diminished the head withdrawal threshold 1 h after the injection compared with vehicle injection (Sidak post hoc test, $P < 0.01$), and this response was blocked by the coinjection of RN-1734 (Sidak post hoc test, $P < 0.05$ for 1 and 2 h; Figure 5(a)). Furthermore, the reduced head withdrawal threshold following elastase injection was also blocked by coinjection of FSLLRY-NH_2 ($n = 5$, $P < 0.01$ for 1 h compared with elastase alone; data not shown). Submucosal injection of FSLLRY-NH_2 or RN-1734 alone did not change head withdrawal threshold ($n = 5$ in each group; data not shown), indicating no anesthetic effects of the drug themselves. These results suggest the occurrence of PAR_2-induced TRPV4-mediated mechanical allodynia following elastase injection into the oral mucosa.

There were no significant differences in the mRNA expression levels of EP_1, PAR_2, TRPV1, TRPA1, and TRPV4 in the trigeminal ganglion between the sham and WiM model (Figure 5(b)), which indicated that expression of the receptors and channels in the WiM model was equivalent to those in naive animals.

Coexpression of TRPV1, TRPA1, and TRPV4

QX-314 is a membrane-impermeable anesthetic, but it passes into the intracellular space via the channel pores of TRPV1 and TRPA1.[35,36] Swab application of 1% QX-314 for 5 min significantly suppressed spontaneous pain in the WiM model (Sidak post hoc test, $P < 0.01$, compared with vehicle; Figure 4(d)), supporting the contributions of continuous TRPV1 and TRPA1 opening to the spontaneous pain mechanism. Despite possible TRPV4 closure during resting conditions (Figure 3(f)), the same application also suppressed the mechanical allodynia (Sidak post hoc test, $P < 0.01$, compared with vehicle; Figure 4(c)). The suppression of mechanical allodynia by QX-314 application was abrogated by the blockade of TRPV1 and TRPA1 following systemic administration of SB-366791 and HC-030031 (Figure 5(c)). These results suggest that TRPV4-mediated mechanical allodynia is suppressed by QX-314 passing through TRPV1 and TRPA1 pore routes rather than the TRPV4 pore.

To confirm the coexpression of TRPV1, TRPA1, and TRPV4 in peripheral nerve fibers, we investigated the Ca^{2+} response to GSK1016790A, AITC, and CPS in dissociated trigeminal ganglion neurons of naive rats. Of 218 neurons from 3 rats that were responsive to high K^+ solution, 164 (75%) showed slowly activated long-lasting Ca^{2+} responses to GSK1016790A, 89 (41%) showed transient Ca^{2+} responses to AITC, and 113 (52%) showed long-lasting Ca^{2+} responses to CPS, as shown in Figure 5(d). In the GSK1016790A-sensitive neurons, 98 (60%) neurons responded to either AITC and/or CPS (Figure 5(e)), indicating that a significant population expressed TRPV4 and TRPV1/TRPA1 in the trigeminal nerve system.

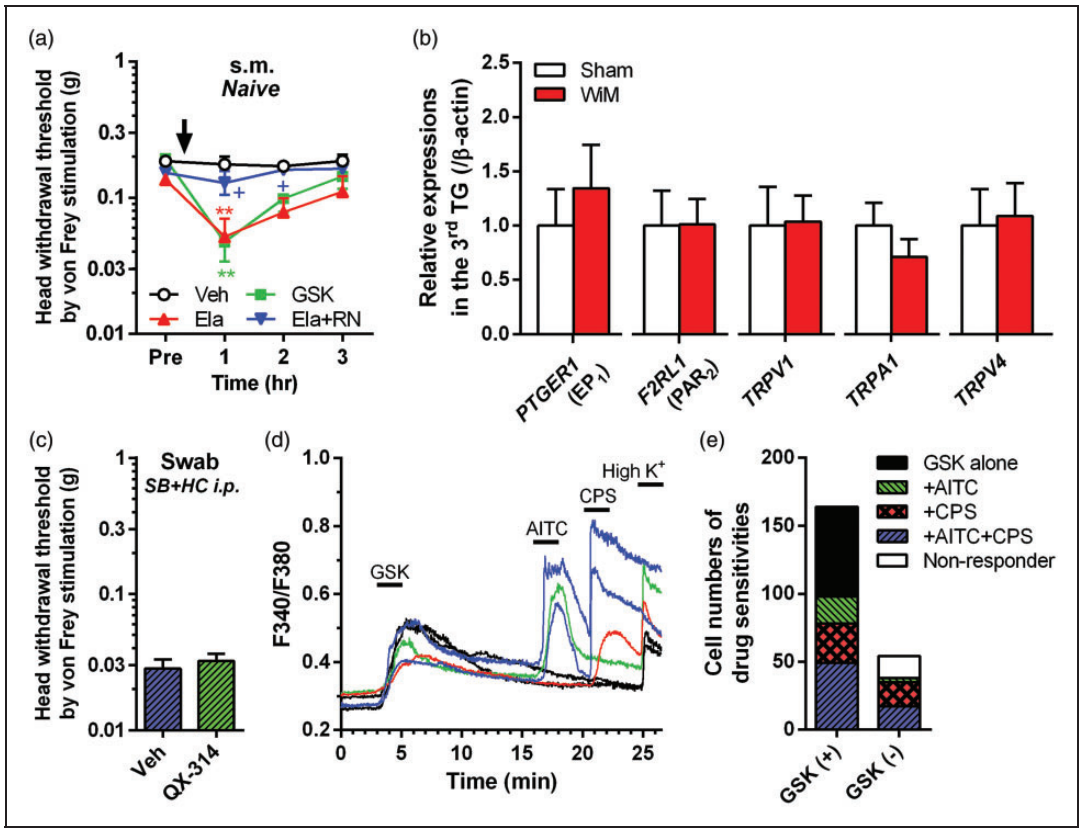

Figure 5. Expression and interaction of pain-related molecules in trigeminal ganglion neurons. (a) TRPV4-mediated mechanical allodynia induction in naive rats. Veh, vehicle (1% ethanol- and 10% dimethylsulfoxide [DMSO]-containing saline; $n = 5$); GSK, GSK1016790A (a TRPV4 agonist; $n = 5$); Ela, elastase ($n = 4$); RN, RN-1734 (a TRPV4 antagonist; $n = 4$). All drugs were injected submucosally (s.m.). $^{**}P < 0.01$ compared with Veh; $^{+}P < 0.05$ compared with Ela alone; Sidak post hoc test following two-way repeated-measures ANOVA. (b) Relative expression levels of *PTGER1* (EP_1 gene), *F2RL1* (PAR_2 gene) *TRPV1*, *TRPA1*, and *TRPV4* in the trigeminal ganglion (TG) of the sham and wire-induced mucositis (WiM) model on day 1 (each group, $n = 4$). (c) Head withdrawal threshold by von Frey filaments after swab application of QX-314 and Veh on day 1 at 30 min after intraperitoneal (i.p.) administration of a mixture of SB-366791 (SB: a TRPV1 antagonist) and HC-030031 (HC: a TRPA1 antagonist) (each group, $n = 6$). (d) Representative Ca^{2+} responses in response to GSK at 100 nM, allyl isothiocyanate (AITC) at 1 mM and capsaicin (CPS) at 1 μM in dissociated trigeminal ganglion neurons of rats. All drugs were applied for 2 min, indicated thick-horizontal bars, by bath application. Data analysis was performed only in CPS- sensitive cells and/or 50 mM KCl solution (High K^{+}) sensitive cells, which are confirmed as neurons. (e) Numbers of AITC and CPS-sensitive cells in GSK-sensitive (+) and -negative (−) neurons ($n = 164$ and 54, respectively). Many GSK (+) neurons were sensitive to either AITC and/or CPS (60%, $n = 98$).

Discussion

The present study is the first report to demonstrate prostanoid- and PAR_2-dependent TRP channel-mediated pain following mechanical trauma in the oral mucosa (Figure 6). The pathophysiological status of the oral traumatic mucositis showed tissue injury-induced inflammation rather than infectious inflammation, together with no efficacy of the antibiotic pretreatment. During dental treatment, iatrogenic oral traumatic mucositis caused by intraoral appliances has received little attention because patient complaints are transient after removal of the injurious parts. However, many patients suffer such trauma-induced pain, leading to poor quality of life and decreased cooperation in therapy.[7,8] The results in this study provide an understanding of the pain mechanism associated with oral traumatic mucositis and effective analgesic approaches for many dental clinicians.

Pathophysiological properties of traumatic oral mucositis

During the one-day installation, repetitive wire-tip attachment to the oral mucosa during jaw movements when eating, drinking, and grooming would induce mechanical inflammation with tissue swelling and generate a traumatic ulcer on the mucosal surface following puncture of the wire-tip. The cellular damage induced leukocyte infiltration and the formation of an abscess

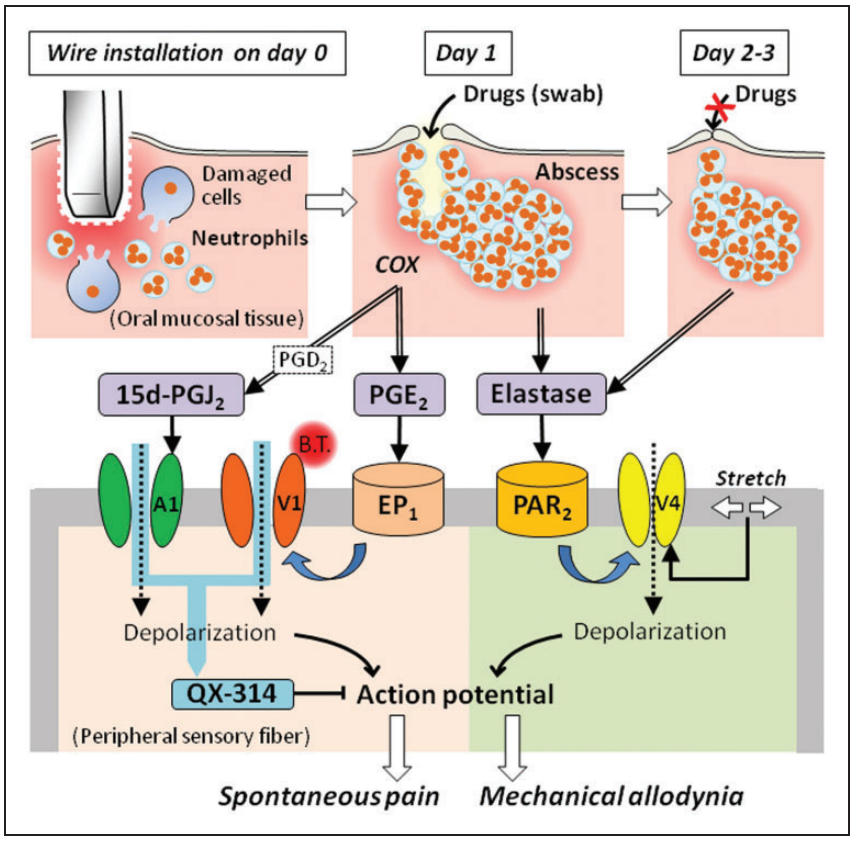

Figure 6. Schematic of the mechanisms underlying oral mucositis-induced pain following mechanical trauma. Following mechanical injury caused by the intraoral appliance, the oral mucosa demonstrates a traumatic ulcer with inflammation that is characterized by leukocyte infiltration due to cell damage. After removing the appliance on day 1, the accumulation of leukocytes forms an abscess below the traumatic ulcer. The ulceration was cured by day 2, but the abscess persisted for a few days. On day 1, proinflammatory cytokines promote prostanoid production in a cyclooxygenase-dependent manner on day 1, and the abscess releases elastase over a longer duration up to days 4 to 5. Arrows with double lines represent chemical release. Prostaglandin E_2 (PGE_2) stimulates EP1, followed by thermal sensitization of TRPV1 on peripheral sensory fibers, resulting in activation at body temperature (B.T.). The cyclopentane prostanoid 15-deoxy-$\Delta^{12,14}$-prostaglandin J_2 (15 d-PGJ_2), which originates from prostaglandin D_2 (PGD_2), directly activates TRPA1 on peripheral sensory fibers, in addition to TRPV1 activation-induced sensitization. Elastase stimulates PAR_2, followed by mechanical sensitization of TRPV4 on peripheral sensory fibers, which is known to be activated by stretch of the cell membrane. Black arrows with solid lines represent agonistic effects of the chemicals on the receptors. Thick blue arrows with twisted lines represent intracellular pathways of TRP channel sensitization. Dashed arrows represent cation influx through channels, resulting in the generation of an action potential following depolarization. QX-314 passes into the intracellular space via the channel pores of TRPV1 and TRPA1, as indicated by a clear blue arrow, and then blocks voltage-dependent sodium channels, providing an anesthetic for both spontaneous pain and mechanical allodynia.

in the submucosal layer until day 1 (Figure 6). The level of phagocytosis by the abundant neutrophils in the injured mucosa was also effective against bacterial infection caused by the traumatic ulcer, maintaining a low infection level. We failed to detect differences in bradykinin, which is the most potent extravasation factor, between healthy oral mucosa and traumatic ulcer on day 1, despite the high level of extravasation in the submucosal layer based on the Evans blue test. The activity of bradykinin was likely completed by day 1 in our model. Using the same analogy, mast cell degranulation in the oral traumatic mucositis seemed to be completed by day 1. Therefore, these pain-producing factors might play an initial role in the inflammatory activity, but not contribute to a large extent after day 1. However, the proinflammatory cytokines, COX-2, PGE_2, and 15 d-PGJ_2, were significantly upregulated on day 1, suggesting their involvements in the pain mechanism in this model.

Prostanoid-dependent TRPV1- and TRPA1-mediated spontaneous pain

Spontaneous pain was inhibited by indomethacin pretreatment, the PGE_2 receptor EP_1 antagonist and TRPV1 and TRPA1-selective antagonists, but not by PAR_2 and TRPV4-selective antagonists. Together with the upregulation of PGE_2 and 15d-PGJ_2 only on day 1, these results suggest that COX-dependent prostanoid

production elicited spontaneous pain through indirect TRPV1 activation following EP_1 activation by PGE_2 and direct TRPA1 activation by 15d-PGJ_2 (Figure 6). Because EP_1 activation has been reported to reduce the thermal threshold of TRPV1 below body temperature through phosphorylation,[32] the sensitized TRPV1 of traumatic mucositis-innervated peripheral fibers would be continuously activated during resting conditions by body temperature. Based on the direct activation of TRPA1 by the cyclopentane prostanoid 15d-PGJ_2,[29] TRPA1 would be activated continuously under resting conditions. The significant efficacy of the membrane-impermeable, TRPV1/TRPA1-permeable anesthetic QX-314 in swab applications supports TRPV1 and TRPA1 channel opening.

The suppression of spontaneous pain following swab application of these antagonists suggests that the spontaneous pain mechanism occurred primarily in the traumatic ulcer region. Spontaneous pain induction and prostanoid upregulation occurred only on day 1 and disappeared by day 2. The timecourse change corresponded to the development and disappearance of traumatic ulcer, suggesting that the painful region within the traumatic mucositis was an ulcer rather than an abscess.

PAR_2-dependent TRPV4-mediated mechanical allodynia

In contrast to spontaneous pain, mechanical allodynia was not suppressed by indomethacin pretreatment and TRPV1 and TRPA1-selective antagonists, in addition to the antioxidative drug and P2X3 and P2X2/3 antagonist. Finally, we observed significant suppression of the PAR_2 receptor antagonist in terms of mechanical allodynia. Based on the complete degranulation of mast cells containing tryptase up to day 1, the serine protease does not seem to contribute to PAR_2 activation. Recently, neutrophil elastase has been reported to sensitize TRPV4 following PAR_2 activation through a distinct intracellular route due to the activation of the representative PAR_2 agonist tryptase.[21] The timecourse of neutrophil elastase upregulation was consistent with those of abscess formation and mechanical allodynia induction. The TRPV4 antagonist significantly suppressed mechanical allodynia on days 1 and 2 by swab application and submucosal injection, respectively. Swab application of the TRPV4 antagonist demonstrated no efficacy on day 2, potentially due to the rapid regeneration of the oral mucosal barrier (Figure 6). Furthermore, in naive rats, submucosal injections of TRPV4 agonist and elastase induced mechanical allodynia, and the elastase-induced mechanical allodynia was blocked by coinjection of TRPV4 or PAR_2 antagonist. These results suggest that elastase released from the abscess elicited mechanical allodynia due to mechanical sensitization of TRPV4 through PAR_2 activation (Figure 6).

The resistance of spontaneous pain to TRPV4 antagonist in the model suggests TRPV4 channel closure during resting conditions and activation only following mechanical stimulation of oral mucositis. Nevertheless, swab application of QX-314 significantly suppressed mechanical allodynia on day 1. No reports have demonstrated the passage of QX-314 through TRPV4 channel pores. After systemic administration of TRPV1 and TRPA1 antagonist, the anesthetic effect of QX-314 on mechanical allodynia disappeared, suggesting that TRPV4-mediated mechanical allodynia was suppressed by the passage of QX-314 through TRPV1 and/or TRPA1 channel pores. In rats and humans, TRPV4 is abundantly expressed in peripheral sensory neurons,[37–39] although its expression in mice is debated.[40–44] In this study, more than 60% of the GSK1016790A-sensitive trigeminal sensory neurons responded to AITC and/or CPS. Taking into consideration the abundant co-expression of TRPV4 and TRPV1/TRPA1, it is likely that the mechanical allodynia-inducible neuronal population partially consisted of a spontaneous pain-inducible subpopulation (Figure 6). However, additional approaches will be required to clear analgesic mechanism of QX-314 in WiM model, for example, electrophysiological experiments for continuous TRPV1/TRPA1 channel opening with QX-314 passing.

Differences in comparison to the infectious oral ulcerative mucositis model

In our previous study using a 5-fluorouracil-administered rat model treated with acetic acid,[10] severe oral ulcerative mucositis with excessive bacterial infection, prostanoid-dependent TRPV1-mediated spontaneous pain, and bacteria toxin-dependent TRPA1-mediated mechanical allodynia were observed, which were largely different from the pain mechanism observed in the WiM model, excluding the efficacy of indomethacin pretreatment for spontaneous pain and mechanical allodynia and the involvement of TRPV1 in spontaneous pain. The administration of 5-fluorouracil induced leukopenia and led to deficient leukocyte infiltration into the injured region, indicating that the activity of neutrophils was largely eliminated. The large difference in the pain mechanism between the models led to differences in bacterial infection levels together with leukocyte functions between the models. In the 5-fluorouracil-administered oral ulcerative mucositis model, lipopolysaccharide and *N*-formyl peptides were derived from extremely infected oral regions that were sensitized to mechanical activation of TRPA1, directly and indirectly via receptor activation.[10] However, in the WiM model, abundant 15 d-PGJ_2 production in traumatic mucositis resulted in continuous TRPA1 channel opening, resulting in spontaneous pain but not mechanical allodynia. Furthermore, the release

of elastase from neutrophils in the abscess elicited TRPV4-mediated mechanical allodynia via PAR_2 activation without activation/sensitization of TRPV1 and TRPA1. Importantly, PAR_2 activation by elastase has been reported to induce mechanical pain but not heat hypersensitivity, which is caused by TRPV1 sensitization.[33]

Clinical significance

The results of this study supply basic scientific evidence for abscess formation in the submucosal layer following the installation of an intraoral appliance in dental patients, as suggested by a clinical review,[6] and indicates that the pathophysiological status of traumatic mucositis is not equivalent to other types of ulcerative mucositis. During dental orthodontic and prosthodontic treatments, the installation of intraoral appliances is needed to improve oral functions during meals and esthetic dentition during conversation. Unfortunately, many dental patients suffer from severe pain in the mechanical lesion caused by the intraoral appliance.[1–4] The pain mechanism underlying traumatic mucositis-induced pain elucidated in this study (Figure 6) suggests that some effective pain treatments will solve pain-related poor quality of life and low cooperation in therapy in dental patients.[7,8] According to the pain relief observed in the WiM model on day 1 following swab applications of various drugs, topical treatments of drug-containing ointment and mouthwash may be effective approaches for patients with mechanically induced ulcerative mucositis. Alternately, systemic oral application of non-steroidal anti-inflammatory agents is also effective for the suppression of spontaneous pain based on the prostanoid dependency of the pain modality in this study. However, the ulcer is quickly healed, but submucosal inflammation, including abscess, persists over subsequent days, suggesting continuation of mechanical allodynia induction in patients following the removal and correction of the injurious parts of orthodontic and prosthodontic appliances. To resolve the continuous pain complaints after being subjected to the intraoral appliance,[1,7,8] systemic administration of PAR_2 antagonistic or neutrophil elastase inhibitory drugs seems to be effective.[34,45]

In conclusion, prostanoids and PAR_2 activation elicit spontaneous pain through TRPV1 and TRPA1 and mechanical allodynia through TRPV4, respectively, independently of bacterial infection, in oral mucositis following mechanical trauma. The pathophysiological pain mechanism suggests that analgesic approaches are effective for dental patients suffering from mucosal trauma-induced pain. To more clarify involvements of TRPV1, TRPA1, and TRPV4 in mucosal trauma-induced pain, it is necessary to perform further genetic approaches (gene knockdown by in vivo siRNA and CRISPR/Cas9 system).

Acknowledgment

The authors thank Dr. Naomi Yada for performing the pathological examinations using histology.

Author contributions

MI, KO, SH, TN, TS, NH, and KY performed animal experiments, biochemical, and molecular biological testing, and Ca^{2+}-imaging and analyzed the data; KO, KG, RH, TK, and KI designed experiments, supervised research, and wrote the manuscript. All authors read and approved the final manuscript.

Declaration of Conflicting Interests

The author(s) declared no potential conflicts of interest with respect to the research, authorship, and/or publication of this article.

Funding

The author(s) disclosed receipt of the following financial support for the research, authorship, and/or publication of this article: This work was supported by a grant-in-aid from the Ministry of Education, Culture, Sports, Science and Technology of Japan (JSPS KAKENHI 16K11483 to KO, 25862027 to KG, and 26861747 to TS).

References

1. Baricevic M, Mravak-Stipetic M, Majstorovic M, et al. Oral mucosal lesions during orthodontic treatment. *Int J Paediatr Dent* 2011; 21: 96–102.
2. Kvam E, Bondevik O and Gjerdet NR. Traumatic ulcers and pain in adults during orthodontic treatment. *Community Dent Oral Epidemiol* 1989; 17: 154–157.
3. Kvam E, Gjerdet NR and Bondevik O. Traumatic ulcers and pain during orthodontic treatment. *Community Dent Oral Epidemiol* 1987; 15: 104–107.
4. Mandali G, Sener ID, Turker SB, et al. Factors affecting the distribution and prevalence of oral mucosal lesions in complete denture wearers. *Gerodontology* 2011; 28: 97–103.
5. Marquezan M, de Freitas AO and Nojima LI. Miniscrew covering: an alternative to prevent traumatic lesions. *Am J Orthod Dentofacial Orthop* 2012; 141: 242–244.
6. Herrera D, Alonso B, de Arriba L, et al. Acute periodontal lesions. *Periodontol 2000* 2014; 65: 149–177.
7. Mansor N, Saub R and Othman SA. Changes in the oral health-related quality of life 24 h following insertion of fixed orthodontic appliances. *J Orthod Sci* 2012; 1: 98–102.
8. Rennick LA, Campbell PM, Naidu A, et al. Effectiveness of a novel topical powder on the treatment of traumatic oral ulcers in orthodontic patients: a randomized controlled trial. *Angle Orthod* 2016; 86: 351–357.
9. Urata K, Shinoda M, Honda K, et al. Involvement of TRPV1 and TRPA1 in incisional intraoral and extraoral pain. *J Dent Res* 2015; 94: 446–454.
10. Yamaguchi K, Ono K, Hitomi S, et al. Distinct TRPV1- and TRPA1-based mechanisms underlying enhancement of oral ulcerative mucositis-induced pain by 5-fluorouracil. *Pain* 2016; 157: 1004–1020.

11. Shapiro H, Singer P and Ariel A. Beyond the classic eicosanoids: peripherally-acting oxygenated metabolites of polyunsaturated fatty acids mediate pain associated with tissue injury and inflammation. *Prostaglandins Leukot Essent Fatty Acids* 2016; 111: 45–61.
12. Honda K, Kitagawa J, Sessle BJ, et al. Mechanisms involved in an increment of multimodal excitability of medullary and upper cervical dorsal horn neurons following cutaneous capsaicin treatment. *Mol Pain* 2008; 4: 59.
13. Harano N, Ono K, Hidaka K, et al. Differences between orofacial inflammation and cancer pain. *J Dent Res* 2010; 89: 615–620.
14. Hitomi S, Ono K, Yamaguchi K, et al. The traditional Japanese medicine hangeshashinto alleviates oral ulcer-induced pain in a rat model. *Arch Oral Biol* 2016; 66: 30–37.
15. Chen Y, Yang C and Wang ZJ. Proteinase-activated receptor 2 sensitizes transient receptor potential vanilloid 1, transient receptor potential vanilloid 4, and transient receptor potential ankyrin 1 in paclitaxel-induced neuropathic pain. *Neuroscience* 2011; 193: 440–451.
16. Omote K, Kawamata T, Nakayama Y, et al. The effects of peripheral administration of a novel selective antagonist for prostaglandin E receptor subtype EP(1), ONO-8711, in a rat model of postoperative pain. *Anesth Analg* 2001; 92: 233–238.
17. Sakamoto A, Andoh T and Kuraishi Y. Involvement of mast cells and proteinase-activated receptor 2 in oxaliplatin-induced mechanical allodynia in mice. *Pharmacol Res* 2016; 105: 84–92.
18. de Oliveira Fusaro MC, Pelegrini-da-Silva A, Araldi D, et al. P2X3 and P2X2/3 receptors mediate mechanical hyperalgesia induced by bradykinin, but not by pro-inflammatory cytokines, PGE_2 or dopamine. *Eur J Pharmacol* 2010; 649: 177–182.
19. Trevisan G, Materazzi S, Fusi C, et al. Novel therapeutic strategy to prevent chemotherapy-induced persistent sensory neuropathy by TRPA1 blockade. *Cancer Res* 2013; 73: 3120–3131.
20. Grace MS, Lieu T, Darby B, et al. The tyrosine kinase inhibitor bafetinib inhibits PAR2-induced activation of TRPV4 channels in vitro and pain in vivo. *Br J Pharmacol* 2014; 171: 3881–3894.
21. Zhao P, Lieu T, Barlow N, et al. Neutrophil elastase activates protease-activated receptor-2 (PAR2) and transient receptor potential vanilloid 4 (TRPV4) to cause inflammation and pain. *J Biol Chem* 2015; 290: 13875–13887.
22. Hitomi S, Ono K, Miyano K, et al. Novel methods of applying direct chemical and mechanical stimulation to the oral mucosa for traditional behavioral pain assays in conscious rats. *J Neurosci Methods* 2015; 239: 162–169.
23. Hidaka K, Ono K, Harano N, et al. Central glial activation mediates cancer-induced pain in a rat facial cancer model. *Neuroscience* 2011; 180: 334–343.
24. Ono K, Harano N, Nagahata S, et al. Behavioral characteristics and c-Fos expression in the medullary dorsal horn in a rat model for orofacial cancer pain. *Eur J Pain* 2009; 13: 373–379.
25. Sago T, Ono K, Harano N, et al. Distinct time courses of microglial and astrocytic hyperactivation and the glial contribution to pain hypersensitivity in a facial cancer model. *Brain Res* 2012; 1457: 70–80.
26. Ono K, Xu S, Hitomi S, et al. Comparison of the electrophysiological and immunohistochemical properties of acutely dissociated and 1-day cultured rat trigeminal ganglion neurons. *Neurosci Lett* 2012; 523: 162–166.
27. Vellani V, Prandini M, Giacomoni C, et al. Functional endothelin receptors are selectively expressed in isolectin B4-negative sensory neurons and are upregulated in isolectin B4-positive neurons by neurturin and glia-derived neurotropic factor. *Brain Res* 2011; 1381: 31–37.
28. Chiu IM, Heesters BA, Ghasemlou N, et al. Bacteria activate sensory neurons that modulate pain and inflammation. *Nature* 2013; 501: 52–57.
29. Materazzi S, Nassini R, Andrè E, et al. Cox-dependent fatty acid metabolites cause pain through activation of the irritant receptor TRPA1. *Proc Natl Acad Sci USA* 2008; 105: 12045–12050.
30. Alessandri-Haber N, Dina OA, Joseph EK, et al. A transient receptor potential vanilloid 4-dependent mechanism of hyperalgesia is engaged by concerted action of inflammatory mediators. *J Neurosci* 2006; 26: 3864–3874.
31. Dall'Acqua MC, Bonet IJ, Zampronio AR, et al. The contribution of transient receptor potential ankyrin 1 (TRPA1) to the in vivo nociceptive effects of prostaglandin E_2. *Life Sci* 2014; 105: 7–13.
32. Moriyama T, Higashi T, Togashi K, et al. Sensitization of TRPV1 by EP1 and IP reveals peripheral nociceptive mechanism of prostaglandins. *Mol Pain* 2005; 1: 3.
33. Lieu T, Savage E, Zhao P, et al. Antagonism of the proinflammatory and pronociceptive actions of canonical and biased agonists of protease-activated receptor-2. *Br J Pharmacol* 2016; 173: 2752–2765.
34. Ossovskaya VS and Bunnett NW. Protease-activated receptors: contribution to physiology and disease. *Physiol Rev* 2004; 84: 579–621.
35. Binshtok AM, Bean BP and Woolf CJ. Inhibition of nociceptors by TRPV1-mediated entry of impermeant sodium channel blockers. *Nature* 2007; 449: 607–610.
36. Brenneis C, Kistner K, Puopolo M, et al. Bupivacaine-induced cellular entry of QX-314 and its contribution to differential nerve block. *Br J Pharmacol* 2014; 171: 438–451.
37. Charrua A, Cruz CD, Jansen D, et al. Co-administration of transient receptor potential vanilloid 4 (TRPV4) and TRPV1 antagonists potentiate the effect of each drug in a rat model of cystitis. *BJU Int* 2015; 115: 452–460.
38. Facer P, Casula MA, Smith GD, et al. Differential expression of the capsaicin receptor TRPV1 and related novel receptors TRPV3, TRPV4 and TRPM8 in normal human tissues and changes in traumatic and diabetic neuropathy. *BMC Neurol* 2007; 7: 11.
39. Qu YJ, Zhang X, Fan ZZ, et al. Effect of TRPV4-p38 MAPK pathway on neuropathic pain in rats with chronic compression of the dorsal root ganglion. *Biomed Res Int* 2016; 2016: 6978923.

40. Alexander R, Kerby A, Aubdool AA, et al. 4α-phorbol 12,13-didecanoate activates cultured mouse dorsal root ganglia neurons independently of TRPV4. *Br J Pharmacol* 2013; 168: 761–772.
41. Chen Y, Kanju P, Fang Q, et al. TRPV4 is necessary for trigeminal irritant pain and functions as a cellular formalin receptor. *Pain* 2014; 155: 2662–2672.
42. Chen Y, Williams SH, McNulty AL, et al. Temporomandibular joint pain: a critical role for Trpv4 in the trigeminal ganglion. *Pain* 2013; 154: 1295–1304.
43. Suzuki M, Mizuno A, Kodaira K, et al. Impaired pressure sensation in mice lacking TRPV4. *J Biol Chem* 2003; 278: 22664–22668.
44. Vandewauw I, Owsianik G and Voets T. Systematic and quantitative mRNA expression analysis of TRP channel genes at the single trigeminal and dorsal root ganglion level in mouse. *BMC Neurosci* 2013; 14: 21.
45. Groutas WC, Dou D and Alliston KR. Neutrophil elastase inhibitors. *Expert Opin Ther Pat* 2011; 21: 339–354.